HHS Public Access

Author manuscript

Nat Cancer. Author manuscript; available in PMC 2022 May 18.

Published in final edited form as:

Nat Cancer. 2021 November ; 2(11): 1124–1135. doi:10.1038/s43018-021-00269-7.

Corresponding Authors: David T. Ting (dting1@mgh.harvard.edu), Massachusetts General Hospital Cancer Center, 149 13th Street, Room 618B, Charlestown, MA 02129, Tel: 617-240-9402, Fax: 617-724-3676; Theodore S. Hong (tshong1@mgh.harvard.edu), Massachusetts General Hospital, Department of Radiation Oncology, 55 Fruit Street, COX3, Boston, MA 02114, Tel: 617-726-6050, Fax: 617-726-3603.

¥These authors contributed equally

*These authors jointly supervised this work

AUTHOR CONTRIBUTIONS

Conceptualization A.R.P., A.S., D.T.T., T.S.H.
Methodology by A.R.P., A.S., M.R., H.T., D.H., A.M., D.J.L., B.D.G., D.T.T., T.S.H.
Formal Analysis by A.R.P., A.S., M.R., H.T., D.H., A.M., D.J.L., B.Y.Y., B.D.G., D.T.T.
Investigation by A.R.P., A.S., M.R., H.T., D.H., A.M., D.J.L., B.D.G., D.T.T., T.S.H.
Resources by A.R.P., J.N.A., J.W.C., J.Y.W., L.C.D., L.S.B., B.J.G., C.D.W., A.X.Z., L.G., R.D.N., J.S.D., N.H., D.P.R., R.B.C., B.D.G., D.T.T., T.S.H.
Data Curation by A.R.P., M.R., D.H., E.E.V., B.E.F., L.E.M., L.L., J.A.M.
Writing – Original Draft by A.R.P., A.S., D.T.T., T.S.H.
Writing – Review & Editing by A.R.P., J.W.C., J.Y.W., A.M., E.E.V., D.P.R., B.Y.Y., R.B.C., B.D.G., D.T.T., T.S.H.
Visualization by A.R.P., A.S., M.R., H.T., A.M., D.J.L., B.Y.Y., D.T.T.
Supervision by A.R.P., A.S., D.T.T., T.S.H.
Project Administration by A.R.P., A.S., E.E.V., L.L., D.T.T., T.S.H.
Funding Acquisition by A.R.P., D.P.R., R.B.C., B.D.G., D.T.T., T.S.H.

COMPETING INTERESTS STATEMENT

A.R.P is a consultant/advisory board member for Eli Lilly, Natera, Checkmate Pharmaceuticals, Inivata, and Pfizer; holds equity in C2I; serves on the DSMC for Roche; and has research funding from Puretech, PMV Pharmaceuticals, Plexxicon, Takeda, BMS, Novartis, Genentech, Guardant, Array, and Eli Lilly.

J.W.C. is author for McGraw Hill and UpToDate.

A.M. is a consultant/advisory board member for Third Rock Ventures, Asher Biotherapeutics, Abata Therapeutics, Rheos Medicines and Checkmate Pharmaceuticals; and holds equity in Asher Biotherapeutics and Abata Therapeutics, which are not related to this work.

C.D.W. is a consultant/advisory board member for Ipsen, Bristol-Myers Squibb and Eli Lilly; and receives research funding from Dicephera, EMD Serono, Ability Pharmaceuticals, Actuate Therapeutics and Novartis.

A.X.Z is a consultant/advisory board member for AstraZeneca, Bayer, Bristol-Myers Squibb, Eisai, Eli Lilly, Exelixis, Merck, Novartis, and Roche/Genentech; research funding from Bayer, Bristol-Myers Squibb, Eli Lilly, Merck, and Novartis.

L.G. is a consultant/advisory board member for Alentis, AstraZeneca, Exelixis, and Sirtex, Genetech, Genentech, H3Biomedicine, Incyte, QED Therapeutics, Servier, and Taiho; and has research funding from Adaptimmune, Bayer, Bristol-Myers Squibb, Eisai, Leap Therapeutics, Loxo Oncology, MacroGenics, Merck, Novartis, Nucana, Relay Therapeutics, Genentech, H3Biomedicine, Incyte, QED Therapeutics, Servier, and Taiho.

N.H. is an advisor and equity holder for Related Sciences, holds equity in BioNTech and receives research funding from Bristol-Meyers Squibb.

D.P.R. is a consultant/advisory board member for MPM Capital, Gritstone Oncology, Oncorus, Maverick Therapeutics, 28/7 Therapeutics, Thrive/Exact Sciences; has equity in MPM Capital, Acworth Pharmaceuticals, and Thrive/Exact Sciences; is a legal consultant for Boeringer Ingelheim; and serves as author for Johns Hopkins University Press, UpToDate, McGraw Hill.

R.B.C. is a consultant/advisory board member for Abbvie, Amgen, Array Biopharma/Pfizer, Asana Biosciences, Astex Pharmaceuticals, AstraZeneca, Avidity Biosciences, BMS, C4 Therapeutics, Chugai, Elicio, Erasca, Fog Pharma, Genentech, Guardant Health, Ipsen, Kinnate Biopharma, LOXO, Merrimack, Mirati Therapeutics, Natera, Navire, N-of-one/Qiagen, Novartis, nRichDx, Remix Therapeutics, Revolution Medicines, Roche, Roivant, Shionogi, Shire, Spectrum Pharmaceuticals, Symphogen, Tango Therapeutics, Taiho, Warp Drive Bio, Zikani Therapeutics; holds equity in Avidity Biosciences, C4 Therapeutics, Erasca, Kinnate Biopharma, nRichDx, Remix Therapeutics, and Revolution Medicines; and has research funding from Asana, AstraZeneca, Lilly, Novartis, and Sanofi.

B.D.G. is a consultant or received honoraria for Darwin Health, Merck, PMV Pharma, ROME Therapeutics, Merck, Bristol–Meyers Squibb, and Chugai Pharmaceuticals; is a founder and has equity in ROME Therapeutics; and has research funding from Bristol-Meyers Squibb.

D.T.T. is a consultant/advisory board member for Pfizer, ROME Therapeutics, Merrimack Pharmaceuticals, Ventana Roche, Nanostring Technologies, Inc., Foundation Medicine, Inc., EMD Millipore Sigma, and Third Rock Ventures, which are not related to this work; is a founder and has equity in PanTher Therapeutics, ROME therapeutics, and TellBio, Inc., which are not related to this work; and has research funding from ACD-Biotechne, PureTech Health LLC, and Ribon Therapeutics, which was not used in this work. D.T.T.'s interests were reviewed and are managed by Massachusetts General Hospital and Mass General Brigham in accordance with their conflict of interest policies.

T.S.H. is consultant/advisory board member for Merck, EMD Serono, PanTher Therapeutics, Boston Scientific, Novocure, and Synthetic Biologics; and has research funding from Taiho, Astra Zeneca, Bristol Myers Squibb, IntraOp, Puma, and Ipsen.

All other authors have no disclosures.

Radiation Therapy Enhances Immunotherapy Response in Microsatellite-stable Colorectal and Pancreatic Adenocarcinoma in a Phase II Trial

Aparna R. Parikh[¥,1,2], **Annamaria Szabolcs**[¥,2], **Jill N. Allen**[1,2], **Jeffrey W. Clark**[1,2], **Jennifer Y. Wo**[3], **Michael Raabe**[2], **Hannah Thel**[2], **David Hoyos**[4], **Arnav Mehta**[2,5], **Sanya Arshad**[2], **David J. Lieb**[5], **Lorraine C. Drapek**[1,2], **Lawrence S. Blaszkowsky**[1,2], **Bruce J. Giantonio**[1,2], **Colin D. Weekes**[1,2], **Andrew X. Zhu**[1,2], **Lipika Goyal**[1,2], **Ryan D. Nipp**[1,2], **Jon S. Dubois**[1,2], **Emily E. van Seventer**[2], **Bronwen E. Foreman**[2], **Lauren E. Matlack**[2], **Leilana Ly**[2], **Jessica A. Meurer**[1,2], **Nir Hacohen**[2,5], **David P. Ryan**[1,2], **Beow Y. Yeap**[1,2], **Ryan B. Corcoran**[1,2], **Benjamin D. Greenbaum**[4], **David T. Ting**[1,2,*], **Theodore S. Hong**[3,*]

[1]Department of Medicine, Division of Hematology & Oncology, Harvard Medical School, Boston, Massachusetts, USA

[2]Massachusetts General Hospital Cancer Center, Harvard Medical School, Boston, Massachusetts, USA

[3]Department of Radiation Oncology, Massachusetts General Hospital, Harvard Medical School, Boston, Massachusetts, USA

[4]Memorial Sloan Kettering Cancer Center, New York, NY 10065, USA

[5]The Broad Institute, Cambridge, MA 02142, USA

Abstract

Overcoming intrinsic resistance to immune checkpoint blockade for microsatellite stable (MSS) colorectal (CRC) and pancreatic (PDAC) cancer remains challenging. We conducted a single-arm, non-randomized, Phase 2 trial (NCT03104439) combining radiation, ipilimumab and nivolumab in patients with metastatic MSS CRC (n=40) and PDAC (n=25) with an ECOG performance status of 0 or 1. The primary endpoint was disease control rate (DCR) by intention to treat. DCR was 25% for CRC (10/40; 95% CI: 13–41%) and 20% for PDAC (5/25; 95% CI: 7–41%). In the per-protocol analysis, defined as receipt of radiation, DCR was 37% (10/27; 95% CI: 19–58%) in CRC and 29% (5/17; 95% CI: 10–56%) in PDAC. Pretreatment biopsies revealed low tumor mutational burden for all samples, but higher expression of NK cells and the HERVK repeat RNA in patients with disease control. This study provides proof-of-concept of combining radiation with immune checkpoint blockade in immunotherapy resistant cancers.

INTRODUCTION

Metastatic colorectal cancer (CRC) and pancreatic ductal adenocarcinoma (PDAC) remains incurable for the vast majority of patients. While significant advances have been made with cytotoxic chemotherapy combinations and to lesser extent biologics in CRC, virtually all patients with unresectable disease will die from the cancer within 5 years[1]. Similarly, while cytotoxic chemotherapy such as FOLFIRINOX has improved short term outcomes in PDAC,

longer term outcomes remain dismal[2]. Immunotherapy represents a promising development in the treatment of cancer but has had limited efficacy in microsatellite stable (MSS) CRC and PDAC[3]. Both single-agent and dual-agent immunotherapy has been tried with limited efficacy (Supplementary Table 1)[4–6]. Most recently, a study of an anti-PD-L1 monoclonal antibody (durvalumab) given as monotherapy or in combination with an anti-CTLA4 monoclonal antibody (tremelimumab) in patients with metastatic PDAC was ineffective with response rates of 0% and 3% respectively[5]. One study with radiation that used a different dosing schedule and sequence when compared to our proposed study showed a response rate of 5%[7]. The only group that reliably responds to immunotherapy are patients with tumors that have microsatellite instability, presumably due to the high mutational rate leading to a large neoantigen burden. In a seminal study by Le and colleagues, patients with mismatch-repair deficient colorectal cancers had a 40% response rate to pembrolizumab. In contrast, no patients with a MSS colorectal cancer responded[3,8]. Similarly, Keynote-158 demonstrated some responses in patients with PDAC, but only in the rare subset of MSI positive patients[9,10].

Radiation therapy has been suggested as a modality that may increase the likelihood of systemic response to immunotherapy via a phenomenon known as the abscopal effect in which local treatment of a tumor leads to antitumor response at distant sites. Mechanistically, pre-clinical data has shown that radiation potentially can increase susceptibility of tumor cells to immune-mediated killing as it has been shown that radiation can increase negative feedback mechanisms such as checkpoints that can hinder the immune response while also promoting release of tumor specific antigens.[11,12–14]. Most recently, data in non-small cell lung cancer demonstrated that treatment with anti-PD1 (pembrolizumab) and stereotactic body radiotherapy doubled out-of-field responses[15]. Previous pre-clinical mouse studies with anti-CTLA4 and radiation identified PD-L1 as a common mechanism of resistance, which could be overcome with anti-PD-L1 therapy[16]. These promising early clinical trials and pre-clinical proof of concept led to this study of combined dual blockade of PD-1 (nivolumab) and CTLA4 (ipilimumab) with radiation therapy in an attempt to stimulate immune responses in metastatic MSS CRC and PDAC.

RESULTS

Efficacy of combined immune checkpoint inhibition and radiation

A total of 40 patients with CRC and 25 patients with PDAC were enrolled in this study (Fig. 1). All patients were confirmed MSS by PCR and/or IHC and had metastatic disease at enrollment. In the CRC cohort, there were 18 women and 22 men with a median age of 59 years (range 26–83). 95% of patients were white, 65% had an ECOG performance status (PS) of 0, median number of prior treatments was 4 (range 1–13). The majority of patients (N=23, 58%) were metastatic at diagnosis and median time from diagnosis to cycle 1 day 1 was 44.9 months (Table 1). In the PDAC cohort, there were 7 women and 18 men: median age, 60 years (range 32–75). 92% of patients were white, 44% had an ECOG PS of 0, median number of prior treatments was 2 (range 1–4). The majority of patients (N=18, 72%) had locally advanced or metastatic disease at diagnosis and median time from diagnosis to cycle 1 day 1 was 16.9 months (Table 1). All patients with PDAC had progressed on

chemotherapy prior to entry and only 1 patient with CRC had stable disease prior to entry but had progressed on 2 prior lines of therapy. Only 1 patient with PDAC had received prior immunotherapy on a previous trial, but this patient did not benefit.

In the 40 CRC patients who enrolled and started treatment, the disease control rate (DCR) was 25% (10/40; 95% CI: 13–41%) with an objective response rate (ORR) of 10% (4/40; 95% CI: 3–24%) by intention to treat (ITT) analysis. The CRC cohort had a median PFS of 2.4 months (95% CI: 1.8–2.5) and median OS of 7.1 months (95% CI: 4.3–10.9)(Fig. 2a,b). Similarly, the 25 PDAC patients had a DCR of 20% (5/25; 95% CI: 7–41%) with an ORR of 12% (3/25; 95% CI: 3–31%) by ITT analysis. Median PFS was 2.5 months (95% CI: 1.6–2.8) with a median OS of 4.2 months (95% CI: 2.1–6.4)(Fig. 2a,b). A total of 34 patients were treated with photons and 12 with protons. In both cohorts, 32% (CRC 13/40; PDAC 8/25) discontinued prior to radiation therapy given autoimmune toxicity leading to clinical decline (N=4), clinical progression (N=7), or progression confirmed by scans (N=10) (Table 2 and Supplementary Table 2). Of the 15 patients who derived clinical benefit, only 1 patient had evidence of some response prior to radiation (Supplementary Table 3).

Four patients in the per-protocol group who received radiation therapy discontinued due to toxicity. In the CRC cohort, adverse events (AEs) related to immunotherapy Grade ≥3 were reported in 70% of patients (53% grade 3, 15% grade 4 and 3% grade 5). The most common Grade ≥3 AEs were lymphopenia and fatigue, and the grade 5 toxicity was pneumonitis (Supplementary Tables 4 and 5). In the PDAC cohort, AEs related to immunotherapy of Grade ≥3 were reported in 56% of patients (44% grade 3, 12% grade 4 and 4% grade 5). The most common Grade ≥3 AEs were lymphopenia, elevated lipase and mucositis. The grade 5 toxicity was hepatic encephalopathy, possibly related to treatment (Supplementary Tables 6 and 7).

In a per-protocol analysis of patients who received radiation therapy, the CRC cohort DCR was 37% (10/27; 95% CI: 19–58%) and ORR was 15% (4/27; 95% CI: 4–34%) and the PDAC cohort DCR was 29% (5/17; 95% CI: 10–56%) and ORR was 18% (3/17; 95% CI: 4–43%). The best objective response as measured from percent change in tumor dimension from baseline are shown as a waterfall plot for CRC (Fig. 3a) and PDAC (Fig. 3b). Only measurable disease outside of the radiation field were evaluated and an example of out of field response in patient 57 is shown by CT scan images of 3 pulmonary metastases shrinking after radiation treatment of the target liver lesion (Fig. 3c). One CRC and one PDAC case had a complete response (CR) by imaging criteria. The patient with CRC presented with metastatic disease after adjuvant therapy for stage III disease and progressed after 4 cycles of FOLFIRI and bevacizumab. She initiated treatment with ipilimumab and nivolumab with radiation to 1 lesion in the liver with a PR at 6 months and a CR 3 months later. However, during treatment she did have a bilateral salpingo-oophorectomy given some question of growth in the ovaries, which did demonstrate metastatic disease. She remained on treatment with a CR and stayed on study for 10 months when she had evidence of new and progressing disease in the liver and peritoneum. The patient with PDAC had widely metastatic disease at presentation. He was started on FOLFIRINOX with approximately 1 year of disease control, and then he was started on trial with RT to the liver lesion with a CR by 5 months. However, he concurrently developed Grade 4 autoimmune

liver toxicity requiring high dose immunosuppression and discontinuation of treatment. He unfortunately progressed seven months after treatment and passed away after a fall leading to an intracranial bleed after 9 months from starting on trial.

The CRC cohort had a median PFS of 2.5 months (95% CI: 2.3–2.8) and median OS of 10.9 months (95% CI: 6.7–15.0) (Fig. 2c,d). Median PFS was 5.2 months (95% CI: 2.5–14.6) for the 10 patients with disease control as best overall response compared to 2.4 months (95% CI: 1.8–2.5) for the 17 without disease control. Median OS was 20.9 months (95% CI: 4.9-not reached) versus 7.7 months (95% CI: 4.0–11.3) for those with and without disease control. In the PDAC cohort, median PFS was 2.7 months (95% CI: 2.5–3.1) and median OS was 6.1 months (95% CI: 4.0–7.0) (Fig. 2c,d). Median PFS was 5.5 months (95% CI: 2.5–7.9) for the 5 patients with disease control as best overall response compared to 2.5 months (95% CI: 1.8–2.8) for the 12 without disease control. Median OS of the per-protocol cohort was 11.7 months (95% CI: 5.4–14.6) versus 4.4 months (95% CI: 3.6–6.4) for those with and without disease control respectively as their best overall response.

Tumor mutational burden and coding gene mutation analysis

Patients underwent biopsies as able prior to trial initiation, immediately prior to radiation treatment, and after radiation completion. A total of 41 tumor samples with paired germline DNA from 17 patients from the per-protocol cohort were analyzed by whole exome sequencing (WES). All patients had low TMB with < 10 mutations/Mb (Fig. 4a and Supplementary Table 8), and there was no difference between patient non-responders (progressive disease = PD) compared to responders (stable disease = SD, partial response = PR, complete response = CR) (Extended Data Fig. 1). Furthermore, there was no change in TMB before, during, or after treatment (Fig. 4a). Analysis of non-synonymous gene mutations identified expected genes that are frequently mutated including *KRAS* and *TP53* mutations in both CRC and PDAC, and common *APC* mutations in CRC (Fig. 4b and Supplementary Tables 9 and 10). In addition, there was notable mutations in DNA damage and repair pathway genes with shared frequent mutations in *DDX11* (CRC 4/13; PDAC 4/10) and *FANCD2* (CRC 2/13; PDAC 2/10). There was no specific DNA damage and repair pathway gene mutation that was particularly enriched in patients with response or disease stability. Notably, patient 4 (CRC PR) and patient 41 (PDAC CR) had 6 mutations in DNA damage and repair genes, which suggests a potential importance of these genes in predicting response, but there were not enough samples in this trial to make any clear conclusions.

Repeat RNA expression associated with disease control

Analysis of pretreatment biopsies comparing patient responders (SD/PR/CR: n = 5) compared to progressive disease (PD: n = 7) revealed coding genes differentially expressed (Fig. 5a and Supplementary Table 11). Gene set overlap analysis showed significant enrichment of epithelial mesenchymal transition (EMT) genes (FDR 2.36 x 10^{-6}) in biopsies from patients with response compared to progressive disease, however, the EMT signature was not uniformly elevated in responders and primarily driven by patients 4, 50, and 51. Closer inspection of the EMT genes differentially expressed noted high *FAP* expression (Fig. 5a) indicating that the signature might be driven by cancer associated fibroblast (CAF) content. Recent single cell RNA-seq analysis of PDAC has revealed heterogeneity

of CAF phenotypes with primarily myofibroblast CAF (myCAF) and inflammatory CAF (iCAF) subtypes reported in human tumors[17–19]. Expression heatmaps for myCAF and iCAF subtypes noted the EMT signature likely being enriched from the elevated presence of myCAFs in patients 4, 50, and 51 (Fig. 5b). De-convolution of immune subsets in RNA-seq data using immune cell transcriptional signatures revealed resting NK cells as being statistically higher in responders compared to progressive disease (unpaired t-test $p = 0.038$; Fig. 5c,d).To evaluate for other potential biomarkers of response, non-coding repeat RNAs were evaluated given their linkage with activation of innate immune receptors and an interferon response in other cancers and model systems[20–24]. Differential expression analysis noted the majority of repeat RNAs were higher in responders compared to progressive disease (Fig. 6a and Supplementary Table 12). After multiple hypothesis correction, there were 5 repeats that were significantly higher (FDR < 0.05) in responders including AluYb9, HERVK, HERV_LTRa, LTR35, and MER34C2 (Fig. 6b). Of these repeats only the HERVK repeat is known to still have protein coding capacity. To evaluate for these markers changing in response to XRT, analysis of paired biopsies pre-XRT and post-XRT RNA-seq was performed and did not identify any significant changes in CAF subtypes, immune subsets, or repeat RNAs (Extended Data Fig. 2). Interestingly, the analysis of the identified pretreatment repeat RNAs noted increased expression post-XRT compared to pre-XRT in the two patients (patient 4 and 33) with objective response, while the patient with stable disease (patient 50) and the progressive disease patients did not see upregulation of repeat RNAs (Fig. 6c). However, the limited numbers of this paired analysis will need future validation. Altogether, the expression of specific repeat elements in pretreatment biopsies and associated elevated resting NK cells is associated with disease control and response in patients who received radiation with combined immune checkpoint blockade.

DISCUSSION

This is a proof-of-concept study demonstrating the safety and modest efficacy of radiation therapy to enhance the effects of dual checkpoint inhibition in MSS metastatic CRC and PDAC. Responses were observed in the group of patients who were able to receive radiation therapy and this contributes to the growing prospective data suggesting radiation therapy may enhance the response rate of immunotherapy[15]. However, what is most notable is the duration of disease control in the patients who had either responses or stable disease. This suggests that using overall response rate to determine efficacy for immunotherapy treatment may perhaps underappreciate the benefit in patients. However, though not directly comparable, the response rate with ipilimumab, nivolumab, and radiation combination still surpasses the single-digit response rates seen with regorafenib or trifluridine and tipiracil in CRC or gemcitabine after FOLFIRINOX in PDAC[25–27]. Toxicity rates in both cohorts were high, but only a small number of patients had clinically relevant toxicity and stopped treatment given toxicity, indicating that toxicity was not limiting and manageable. There was one CRC patient with grade 5 pneumonitis, but this patient also had a substantial degree of underlying lung disease which may have also been contributory and in the PDAC cohort there was one grade 5 hepatic encephalopathy in a patient with extensive liver disease with

concomitant hepatotoxicity from immunotherapy. Despite the modest activity, any activity in this subset of MSS patients with CRC and PDAC warrants further evaluation.

There was notable early dropout (progression, toxicity, declining PS) in this trial as a third of patients in both cohorts never had the opportunity to receive radiation and current ongoing trials are addressing this dropout whereby radiation is moved to the start of treatment. Alternative dosing schedules for the integration of radiation with immunotherapy might be more active as the extent of immune-modulation with varying dosing and fractionating radiation therapy is still not well understood and continues to be under investigation[28–30]. For example, recent data suggests that PD-1 blockade prior to antigen priming leads to T-cell exhaustion given the induction of dysfunctional $CD8^+$ cells by PD-1 blockade.[31] Therefore, concurrent priming may be optimal in preventing the induction of dysfunctional CD8 cells and the sequencing in this study (with anti-PD1 therapy given for 3 doses before radiation therapy was delivered) may have been suboptimal. In the future, it will be critical to consider modifications to the dosing schedule to accommodate radiation upfront as well as modifications that mitigate the toxicity seen.

Although the exact mechanism for response from this approach is not fully understood, pre-clinical models have indicated that radiation enhances the diversity of T-cell receptor (TCR) repertoire in intratumoral T-cells and increases dendritic cell infiltration and antigen presentation in the tumor[16,28,32–34]. Analysis of biopsies for potential genomic predictive biomarkers of response noted all tumors had low TMB and there were no clear mutations associated with response. Although a couple of patients with response had tumors with multiple mutations in DNA damage and repair pathway genes, there was no consistent pattern of response as has been recently demonstrated in a larger series of tumors treated by immune checkpoint inhibitors[35]. Analysis of the transcriptome demonstrated significant expression of multiple repeat RNAs with associated higher resting NK cells in pretreatment biopsies from patients with disease control or response. These findings are consistent with previous reports showing a relationship of repeat RNA expression and response to immune checkpoint inhibitors[22,36]. Moreover, previous work has also observed a correlation of cytolytic activity and NK cells with the expression of HERV RNA species[37,38] consistent with our findings. Although there are a variety of repeat RNAs elevated in pancreatic and colorectal cancers that have been reported, there appears to be clear distinct expression pattern of this wide spectrum of repeat RNAs that are associated with different epigenetic and immunologic features of these cancers[36,39–42]. For example, the specific elevation of the endogenous retrovirus HERVK in responders is consistent with our previously reported correlation of this particular repeat RNA with immune checkpoint response in urothelial carcinoma[36]. Others have also found HERV expression associated with immune checkpoint response in renal cell carcinoma, which is thought to be a combination of enhanced innate immune response from HERV RNA species and potential adaptive immune response to protein coding elements of these ancient retrovirsues[37,43]. Similarly, NK cells have become recognized as a potential effector cell for anti-PD-1/PD-L1 therapies[44,45]. NK cell expression of PD-1 has been demonstrated in these studies and anti-PD-1 therapies can activate these innate immune cell effectors along with adaptive cytolytic T-cells for a full anti-tumoral immune response. Altogether, this indicates that specific repeats are associated with differences in NK cell infiltrates that can be used as potential biomarkers

of immune checkpoint inhibitor trials. The functional relationship of these repeat RNAs on innate immune sensing pathways and associated immune cell response is an underdeveloped area of research that merits further investigation.

The addition of radiation therapy to PD-1 and CTLA4 pathway inhibition has demonstrated some activity in otherwise refractory CRC and PDAC patients for whom dual PD-1 and CTLA4 pathway inhibition historically has had limited activity. Though modest, duration of disease control and clinical benefit was notable in this human proof of concept study, warranting further investigation in a confirmatory study. Furthermore, given the high level of early-drop out in this trial as well as new information on potential improved timing of the sequencing of radiation therapy with immunotherapy to enhance efficacy, follow up studies with a different treatment schedule, including moving the radiation treatment to earlier in the treatment course, are planned. Finally, repeatome gene expression profiling can serve as a source of potential predictive biomarkers of immunotherapy and provide new targets for mechanistic studies in understanding the role of these viral like sequences in cancer biology.

METHODS

Data Availability Statement

All RNA-seq data has been uploaded to NCBI GEO accession GSE179351 and whole exome sequencing has been uploaded to NCBI dbGaP accession phs002545.v1.p1.

Source data for Fig. 2, 3, 4, 5, 6 and Extended Data Fig. 1, 2 have been provided as Source Data files. All other data supporting the findings of this study are available from the corresponding author on reasonable request.

Code Availability Statement

There was no custom code developed for this project, but all code and statistical packages used for the study will be provided upon request. For whole exome sequencing, the following software resources were used: GATK b37 resource bundle (https://gatk.broadinstitute.org/hc/en-us/articles/360035890811-Resource-bundle), picard-2.11.0 MarkDuplicates (http://broadinstitute.github.io/picard), bam-readcount software (0.8.0-unstable-6–963acab-dirty (commit 963acab-dirty); https://github.com/genome/bam-readcount), and snpEff.v4.3t software. Additional details for whole exome sequencing can be found at https://github.com/dfhoyosg/17–021_RT_IpiNivo. For RNA-seq, the following software resources were used: STAR aligner (Version 2.7.7), DESeq2 (Version 1.32.0), and CIBERSORTx.

Trial Registration: Nivolumab and Ipilimumab and Radiation Therapy in Microsatellite Stable (MSS) and Microsatellite Instability (MSI) High Colorectal and Pancreatic Cancer. Registration #NCT03104439. https://clinicaltrials.gov/ct2/show/NCT03104439?term=17-021&rank=1.

Patient Selection

Metastatic MSS Colorectal Cancer—Eligibility criteria included; at least 18 years old; histologically or cytologically confirmed adenocarcinoma of colorectal documented as MSS by PCR and/or IHC; Eastern Cooperative Oncology Group performance status ≤1; life expectancy of greater than 3 months; adequate hematologic function (absolute neutrophil count ≥ 1000/mcL, white blood count ≥ 2000/mcL, platelets ≥ 75,000/mcL, hemoglobin ≥ 7.5 g/dL); adequate renal function (serum creatinine ≤1.5 the upper limit of normal or creatinine clearance ≥ 40ml/min); adequate hepatic function (serum total bilirubin ≤ 1.5 the upper limit of normal, AST and ALT ≤3 the upper limit of normal or ≤ 5 the upper limit of normal in patients with liver metastases; adequate coagulation (International Normalized Ratio or Prothrombin Time (PT) ≤ 1.5 X ULN and Activated Partial Thromboplastin Time (aPTT) ≤ 2.5 X ULN; participants must have been on a stable dose of dexamethasone 2 mg or less for 7 days prior to initiation of treatment. Participants were also required to have one previously unirradiated lesion to serve as the radiotherapy target lesion amenable to a prescribed dose of 8 Gy x 3 which would meet dose constraints, and another unirradiated measurable lesion > 1 cm in size outside the radiation field that could be used as measurable disease; documentation of microsatellite status; patients must have received prior fluorouracil (5FU), irinotecan and oxaliplatin (any combination) or have a contraindication to receiving these agents. Exclusion criteria include participants who had received chemotherapy, targeted small molecule therapy or study therapy within 14 days of protocol treatment, or those who have not recovered [i.e., ≤ Grade 1 (or ≤ Grade 2 for neuropathy) or at baseline] from adverse events due to agents administered more than 2 weeks earlier. Subjects with major surgery must have recovered adequately; participants currently receiving any other investigational agents; known or suspected autoimmune disease other than vitiligo, type I diabetes mellitus, residual hypothyroidism due to autoimmune condition only requiring hormone replacement, psoriasis not requiring systemic treatment, or conditions not expected to recur in the absence of an external trigger condition requiring systemic treatment with either corticosteroids (> 10 mg daily prednisone equivalents) or other immunosuppressive medications within 14 days of study drug administration); prior systemic treatment with an anti-CTLA4 antibody, anti-PD1 or PDL1 antibody; known history of active TB, HBV, HCV or HIV; uncontrolled intercurrent illness or psychiatric illness/social situations that would limit compliance with study requirements; pregnant or breastfeeding; known additional malignancy that is progressing or requires active treatment (excluding basal cell carcinoma of the skin and squamous cell carcinoma of the skin that has undergone potentially curative therapy or in situ cervical cancer); known history of, or any evidence of active, non-infectious pneumonitis; active infection requiring systemic therapy; received a live vaccine within 30 days of planned start of study therapy; history of allergy to study drug components; history of severe hypersensitivity reaction to any monoclonal antibody; uncontrolled brain metastases (patients treated with radiation ≥ 4 weeks prior with follow up imaging showing control were eligible).

Metastatic MSS Pancreatic Ductal Adenocarcinoma—Inclusion criteria was identical to MSS CRC cohort except for the following differences: histologically or cytologically confirmed adenocarcinoma of pancreas, patients could receive treatment after

progressing on one or more lines of therapy, and documentation of microsatellite status was required but did not preclude eligibility. Exclusion criteria also were identical to the MSS cohort of included participants except in the PDAC cohort, patients could have received prior PD-1 or PDL-1 inhibitors. All procedures were conducted in accordance with the Declaration of Helsinki and the International Conference on Harmonization Guidelines for Good Clinical Practice.[46] The protocol and all amendments were reviewed by the scientific review committee and institutional review board at the Dana Farber Cancer Institute/Harvard Cancer Center. All patients provided written informed consent prior to enrollment.

Study Design and Treatment

This was an open-label, single-arm, Phase 2 clinical trial conducted at the Massachusetts General Hospital (MGH) Cancer Center in Boston, MA. Patients enrolled between 07/2017 to 12/2018. On cycle 1, day 1, patients received one dose of nivolumab 240 mg and ipilimumab 1 mg/kg. Nivolumab was administered first as a 30-minute IV infusion followed by ipilimumab, as a 30-min IV infusion, 30 minutes after completion of the nivolumab infusion. Patients went on to receive nivolumab 240 mg once every two weeks, on days 15, 29 of a 42-day cycle. On cycle 2, day 1, patients again received nivolumab 240 mg and ipilimumab 1 mg/kg but also started radiation. Patients received 24 Gy total given as 3 fractions of 8 Gy administered every other day or 2 days as needed. All treatments were administered at either the Clark Center for Radiation Oncology or the Francis H. Burr Proton Center at MGH. After radiation, treatment continued with receive nivolumab 240 mg days every two weeks, on days 15, 29 of a 42-day cycle. For cycle 3 and beyond, patients continued treatment with ipilimumab 1 mg/kg on day 1 with nivolumab 240 mg and then nivolumab every two weeks for a 42 day cycle until disease progression defined according to Response Evaluation Criteria in Solid Tumors version 1.1[47], unacceptable toxicity, or withdrawal. Dose interruptions and management of immunologic toxicities were in accordance with the protocol.

Correlative Science

Optional biopsies of the tumor site being radiated were done prior to treatment, immediately prior to radiation (weeks 2–5) and within 2 weeks after radiation completion. Whole blood was obtained from patients for DNA germline control. RNA and genomic DNA was extracted from fresh frozen biopsies after homogenization with a TissueLyser (2x4 minutes at 20Hz), using the Qiagen AllPrep DNA/RNA/Protein mini kit (Cat.No.80004, Qiagen) according to manufacturer instructions. Germline genomic DNA was extracted from whole blood samples with the use of the DNAzol BD reagent (10974020, Invitrogen).

Whole Exome Sequencing (WES)—A total of 41 tumor samples with paired germline DNA from 17 patients from the per-protocol cohort were analyzed by WES. The Nextera DNA Exome kit (20020617, Illumina) was used to prepare pooled libraries enriched in exonic regions. A genomic DNA input of 50 ng was used per sample. After library preparation and amplification (10 cycles), up to 8 dual indexed libraries were pooled together for the downstream enrichment steps. Pooled samples were sequenced using on a HiSeq X using 150–150 paired end reads.

Whole Exome Sequencing analysis—We called single nucleotide variations (SNVs) and indel mutations from paired-end whole-exome sequencing reads, for which read lengths were 150 base pairs. We downloaded the Broad Institute's GATK b37 resource bundle (https://gatk.broadinstitute.org/hc/en-us/articles/360035890811-Resource-bundle) as reference data for read processing. We pre-processed sequencing reads according to GATK Best Practices recommendations[48,49].

We first aligned the sequencing reads to the human_g1k_v37_decoy reference genome (GRCh37) using bwa-0.7.17 mem [50] and samtools-1.6[51]. Duplicates were marked with picard-2.11.0 MarkDuplicates (http://broadinstitute.github.io/picard). Indel realignments were done with the Genome Analysis toolkit (GenomeAnalysisTK-3.8–1-0-gf15c1c3ef) RealignerTargetCreator and IndelRealigner[52] using the 1000 genome phase1 indel (1000G_phase1.indels.b37.vcf) and Mills indel calls (Mills_and_1000G_gold_standard.indels.b37.vcf) as references. Base calls were recalibrated with BaseRecalibrator[52] and dbSNP version 138.

MuTect 1.1.7[53] and Strelka 1.0.15[54] were used to call SNVs and indels on pre-processed sequencing data. For the MuTect calls, dbSNP 138 and CosmicCodingMuts.vcf version 86[55] were used as reference files. For the Strelka calls, we set "isSkipDepthFilters = 1" to prevent filtering-out of mutation calls from exome sequencing due to exome-sequencing mapping breadth.

Unbiased normal/tumor read counts for each SNV and indel call were then assigned with the bam-readcount software (0.8.0-unstable-6–963acab-dirty (commit 963acab-dirty); https://github.com/genome/bam-readcount). A minimum base quality filter of "-b 15" was used for all mutations except for possible KRAS mutations, which instead had no such filter. This was to capture all possible driver KRAS mutations. The reads were counted in an insertion-centric way with the "-i" flag, so that reads overlapping with insertions were not included in the per-base read counts. of The union of all mutation calls were annotated with the snpEff.v4.3t software[56] using the following code:

```
$java_path -jar $snpeff_path ann \
-noStats \
-strict \
-hgvs1LetterAa \
-hgvs \
-canon \
-fastaProt $output_path/"$vcf_name"".fasta" \
GRCh37.75 \
$input_vcf \
> $output_path/"$vcf_name""_ann.vcf"
```

Only annotations without "WARNING" or "ERROR" were kept.

Common mutations in KRAS known to be pathogenic were then manually curated (chromosome 12, bases 25378562, 25380275, 25398281, 25398282, 25398284, and 25398285) corresponding to the top ten coding mutations in KRAS denoted in the Genomic Data Commons Database[57] if the sample already did not already contain a KRAS mutation. Five additional KRAS mutations were added in this way.

Tumor mutational burden (TMB) was computed for: (1) all mutations, (2) nonsynonymous SNV mutations, and (3) missense mutations. Coding mutations with variant allele frequencies greater than 10% were reported as “high-quality”. All KRAS mutations were reported.

Statistical Analysis—Statistical analysis of TMB between samples were calculated using an unpaired t-test between PD versus SD/PR/CR. Paired t-test and a mixed-effects analysis with the Geisser-Greenhouse correction were performed on pretreatment, pre-XRT, and post-XRT samples from the same patients.

Total RNA sequencing (RNA-seq)—The Smarter Stranded Total RNA-Seq kit v2 (634413, Takara) was used with 10 ng RNA input and 4 minutes fragmentation time, according to the manufacturer instructions to generate dual-indexed libraries for total RNA sequencing. After qPCR-based quantification (KAPA library quantification kit, 07960140001, Roche), libraries were pooled and sequenced on the Illumina NextSeq 500 platform using a 150 cycles kit with paired end read mode.

RNA-seq computational analysis—Raw Illumina reads were quality-filtered as follows. First, ends of the reads were trimmed to remove N’s and bases with quality less than 20. After that, the quality scores of the remaining bases were sorted, and the quality at the 20th percentile was computed. If the quality at the 20th percentile was less than 15, the whole read was discarded. Also, reads shorter than 40 bases after trimming were discarded. If at least one of the reads in the pair failed the quality check and had to be discarded, we discarded the mate as well.

Quality filtered reads were mapped to the human genome (gencode annotation, build 38) and to repbase elements (release 20) using STAR aligner. Aligned reads were assigned to genes using the featureCounts function of the Rsubread package using the external Ensembl annotation. This produced the raw read counts for each gene. Mapping and counting of the reads was done in 2 stages. First, reads were mapped to the human genome, and the counts were determined using the Gencode annotation and the annotation derived from the repeatmasker output. After that, the reads which were not assigned to any feature in either Gencode and repeatmasker annotation were realigned to the repeat consensus sequence (repbase). Counts obtained from repeatmasker and repbase were added together.

Differential Gene Expression Analysis—Differential expression and statistical analysis were performed using DESeq2 in R, with un-normalized raw read counts as the input. A false discovery rate (FDR) adjusted p value < 0.05 was used for the selection of differentially expressed genes. For repeat RNA analysis, all tRNA, rRNA, and simple repeats were removed before differential expression. All un-normalized raw read counts

for genes and repeats were used for DESeq2 normalization and differential expression performed only on repeat genes. For coding genes, only un-normalized raw read counts for protein coding genes were used for input for DESeq2 normalization and differential expression performed. Before plotting, repeat RNA and coding genes were normalized to total protein coding counts as reads per million (RPM) + 1 for log2 transformation (log2(RPM+1)). Rescaled heatmaps for expression are shown with 2 and −2 set as the maximum and minimum values of the dataset shown. Cell type deconvolution from gene expression was performed using CIBERSORTx[58] using the LM22 signature matrix and batch correction for bulk sorted reference profiles. Heatmaps of cell percentage were generated in PRISM 9 for MacOS. Statistical analysis of cell percentages between samples were calculated using an unpaired t-test between PD versus SD/PR/CR.

Assessments

Participants were seen weekly for clinical assessments including a physical examination with vital signs, performance status, hematology, and biochemistry tests on or within 72 hours before Day 1, then weekly until week 12, and subsequently every two weeks. Participants were evaluated for radiographic response every 12 weeks, noting that the first scan was performed after completion of radiation. In addition to a baseline scan, confirmatory scans were obtained 3 weeks following initial documentation of objective response. Scans could also be obtained prior to every 12 weeks at the clinician's request. Patients were followed for survival until death, withdrawal of consent for follow-up or up to 5 years. All AEs were monitored from registration until 30 days after treatment and were graded according to the National Cancer Institute Common Terminology Criteria for Adverse Events, Version 4.03. Following disease progression, patients were followed-up within 30 days from the last dose +/− 7 days or coinciding with the date of discontinuation (+/− 7 days) if date of discontinuation was greater than 37 days after last dose with a second follow-up visit 8–10 weeks (+/− 7 days) from follow-up visit 1. After 2 in person follow-up visits, patients were followed with a phone call or in clinic visit every 10–12 weeks for survival.

Study End Points

The primary trial endpoint was disease control rate (response plus stable disease [DCR]) by RECIST 1.1. Responses and stable disease were defined as responses and stability outside of the irradiated field. Secondary endpoints include overall response rate (complete response and partial response [ORR]) in unirradiated lesions, treatment-related adverse event (AE) rates, overall survival (OS) and progression-free survival (PFS). Exploratory objectives included biomarker analysis of serial tumor biopsies and peripheral blood samples.

Statistics & Reproducibility

Clinical Trial—A two-stage design was used to demonstrate a DCR of 20% under the alternative hypothesis as the minimum level of promising efficacy, while a 5% rate is specified under the null hypothesis to indicate minimal or no activity. In the MSS cohort if at least 2 of the first 20 patients achieved disease control, the cohort proceeded to enroll a total of 40 patients. The two-stage design provided 92% power to accept the protocol

treatment is associated with a 20% rate of disease control if at least 4 of 40 patients achieved disease control, while the probability of a type 1 error is 10% if the underlying rate of disease control were truly only 5%. In the mPDAC cohort if at least 1 of the first 15 patients achieved disease control, the cohort proceeded to enroll a total of 25 patients. The two-stage design provided 89% power to accept the protocol treatment is associated with a DCR of 20% if at least 3 of 25 patients achieved disease control, while the probability of a type 1 error is 12% if the underlying DCR were truly only 5%. DCR and ORR were reported with the 95% confidence interval (95% CI) based on the exact binomial distribution. PFS and OS were measured from the first dose of protocol treatment. PFS was defined as time until the earlier date of either progressive disease or death, or otherwise censored at the date of last follow-up. OS was defined as time to death from any cause or otherwise censored at the date of last follow-up for patients still alive at the time of analysis. OS and PFS curves were estimated by the Kaplan-Meier method, with the 95% CI obtained by the log-log transformation. Primary analysis was based on the intention-to-treat (ITT) population, while the per-protocol analysis was defined in patients who received radiation. Statistical analyses were performed using SAS version 9.4 (SAS Institute, Cary, NC) and R version 3.3.1 (R Foundation).

Correlative Science—All statistics for DNA and RNA sequencing is detailed above. Statistical analysis using t-test were performed using GraphPad Prism version 9.1.2. as specified in the legend or methods above.

Extended Data

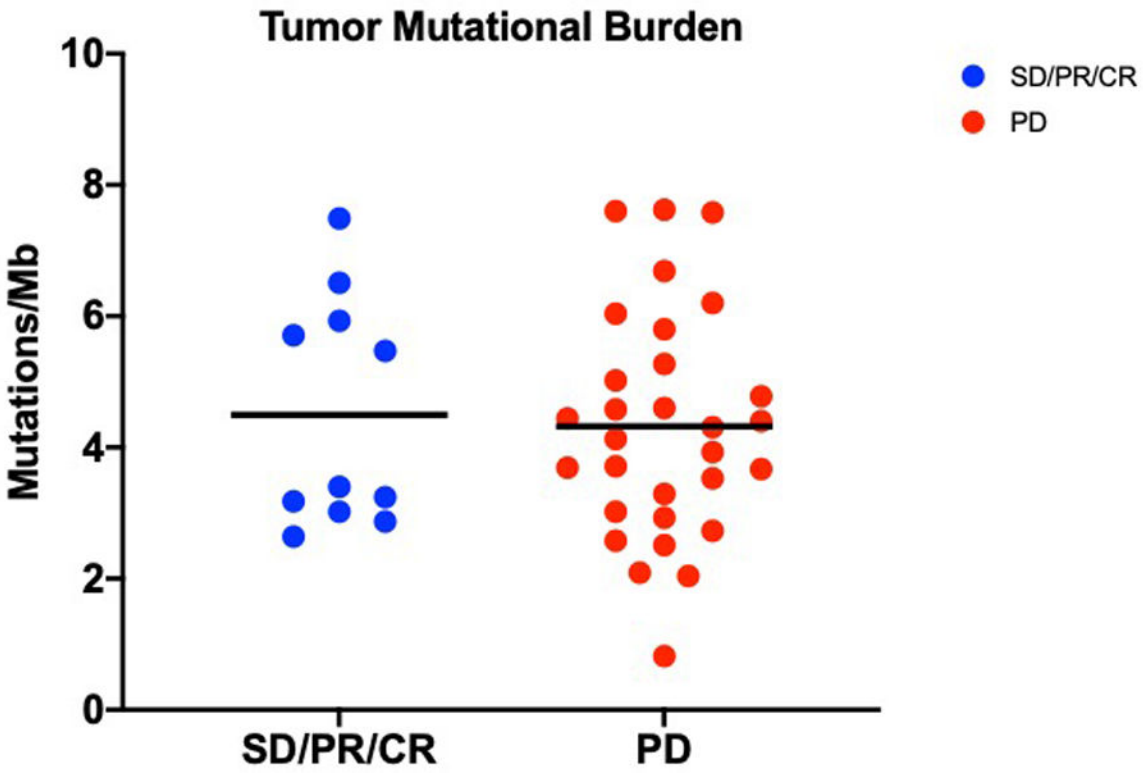

Extended Data Fig. 1. Tumor Mutational Burden of all samples between responders and progressive disease.

Mutations per megabase shown with mean (bar) for patients with SD/PR/CR (n = 5) or PD (n = 12). Unpaired 2-tailed t-test p = 0.7738 was not significant.

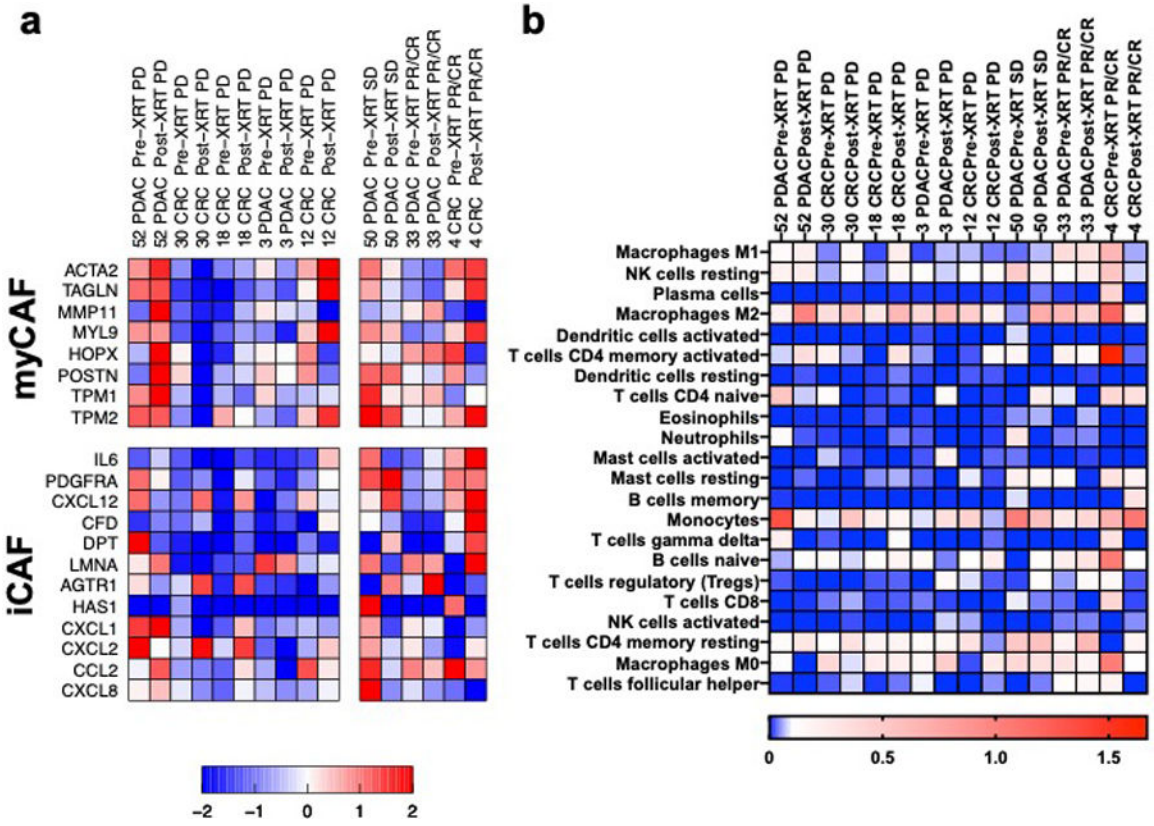

Extended Data Fig. 2. Expression analysis of paired pre-XRT and post-XRT biopsy samples.

a, Heatmap of cell RNA-seq expression of myCAF and iCAF in pre-XRT and post-XRT biopsies from patients with SD/PR/CR (n = 3) and PD (n = 5). Scale −2 to 2 represents minimum and maximum values within the heatmap. **b**, Heatmap of cell percentage of immune cells in pre-XRT and post-XRT biopsies from patients with SD/PR/CR (n = 3) and PD (n = 5).

Supplementary Material

Refer to Web version on PubMed Central for supplementary material.

ACKNOWLEDGEMENTS

We are grateful to Sasha Solovyov for his help in computational and statistical consultation for this project.
This work was supported by SU2C-AACR-DT22–17 Colorectal Dream Team: Targeting Genomic, Metabolic, and Immunological Vulnerabilities of Colorectal Cancer (A.R.P., R.B.C., D.T.T., T.S.H.); National Institutes of Health grants P50CA127003 (R.B.C.), R01CA240924 (D.T.T., B.D.G.), U01CA228963 (D.T.T., B.D.G.); Conquer Cancer Foundation ASCO CDA (A.R.P.); SU2C and Lustgarten Foundation (D.P.R., B.D.G., D.T.T., T.S.H.); The Robert L. Fine Cancer Research Foundation (D.T.T.); and generous donations from David and Ingrid Kosowsky, Sandra and Arthur Irving, and Robert and Marian Ettl.

REFERENCES

1. https://www.cancer.org/cancer/colon-rectal-cancer/about/key-statistics.html. Accessed June 17, 2019.
2. Conroy T et al. FOLFIRINOX versus gemcitabine for metastatic pancreatic cancer. N Engl J Med 364, 1817–1825, doi:10.1056/NEJMoa1011923 (2011). [PubMed: 21561347]
3. Le DT et al. Mismatch-repair deficiency predicts response of solid tumors to PD-1 blockade. Science (New York, N.Y.) 357, 409–413, doi:10.1126/science.aan6733 (2017).
4. Chung KY et al. Phase II study of the anti-cytotoxic T-lymphocyte-associated antigen 4 monoclonal antibody, tremelimumab, in patients with refractory metastatic colorectal cancer. J Clin Oncol 28, 3485–3490, doi:10.1200/jco.2010.28.3994 (2010). [PubMed: 20498386]
5. O'Reilly EM et al. Durvalumab With or Without Tremelimumab for Patients With Metastatic Pancreatic Ductal Adenocarcinoma: A Phase 2 Randomized Clinical Trial. JAMA Oncol, doi:10.1001/jamaoncol.2019.1588 (2019).
6. Chen EX et al. Effect of Combined Immune Checkpoint Inhibition vs Best Supportive Care Alone in Patients With Advanced Colorectal Cancer: The Canadian Cancer Trials Group CO.26 Study. JAMA Oncology 6, 831–838, doi:10.1001/jamaoncol.2020.0910 (2020). [PubMed: 32379280]
7. Xie C et al. Immune Checkpoint Blockade in Combination with Stereotactic Body Radiotherapy in Patients with Metastatic Pancreatic Ductal Adenocarcinoma. Clinical Cancer Research 26, 2318–2326, doi:10.1158/1078-0432.Ccr-19-3624 (2020). [PubMed: 31996388]
8. Le DT et al. PD-1 Blockade in Tumors with Mismatch-Repair Deficiency. New England Journal of Medicine 372, 2509–2520, doi:doi:10.1056/NEJMoa1500596 (2015).
9. Marabelle A et al. Efficacy of Pembrolizumab in Patients With Noncolorectal High Microsatellite Instability/Mismatch Repair-Deficient Cancer: Results From the Phase II KEYNOTE-158 Study. J Clin Oncol 38, 1–10, doi:10.1200/jco.19.02105 (2020). [PubMed: 31682550]
10. Hu ZI et al. Evaluating Mismatch Repair Deficiency in Pancreatic Adenocarcinoma: Challenges and Recommendations. Clin Cancer Res 24, 1326–1336, doi:10.1158/1078-0432.Ccr-17-3099 (2018). [PubMed: 29367431]
11. Jiang W, Chan CK, Weissman IL, Kim BYS & Hahn SM Immune Priming of the Tumor Microenvironment by Radiation. Trends in cancer 2, 638–645, doi:10.1016/j.trecan.2016.09.007 (2016). [PubMed: 28741502]
12. Deng L et al. Irradiation and anti-PD-L1 treatment synergistically promote antitumor immunity in mice. The Journal of clinical investigation 124, 687–695, doi:10.1172/jci67313 (2014). [PubMed: 24382348]
13. Formenti SC et al. Radiotherapy induces responses of lung cancer to CTLA-4 blockade. Nature medicine 24, 1845–1851, doi:10.1038/s41591-018-0232-2 (2018).
14. Kroemer G, Galluzzi L, Kepp O & Zitvogel L Immunogenic cell death in cancer therapy. Annu Rev Immunol 31, 51–72, doi:10.1146/annurev-immunol-032712-100008 (2013). [PubMed: 23157435]
15. Theelen WSME et al. Effect of Pembrolizumab After Stereotactic Body Radiotherapy vs Pembrolizumab Alone on Tumor Response in Patients With Advanced Non–Small Cell Lung Cancer: Results of the PEMBRO-RT Phase 2 Randomized Clinical TrialPembrolizumab Alone vs After Stereotactic Body Radiotherapy in Patients With Advanced NSCLCPembrolizumab Alone vs After Stereotactic Body Radiotherapy in Patients With Advanced NSCLC. JAMA Oncology, doi:10.1001/jamaoncol.2019.1478 (2019).
16. Twyman-Saint Victor C et al. Radiation and dual checkpoint blockade activate non-redundant immune mechanisms in cancer. Nature 520, 373–377, doi:10.1038/nature14292 (2015). [PubMed: 25754329]
17. Ohlund D et al. Distinct populations of inflammatory fibroblasts and myofibroblasts in pancreatic cancer. J Exp Med 214, 579–596, doi:10.1084/jem.20162024 (2017). [PubMed: 28232471]
18. Biffi G et al. IL1-Induced JAK/STAT Signaling Is Antagonized by TGFbeta to Shape CAF Heterogeneity in Pancreatic Ductal Adenocarcinoma. Cancer Discov 9, 282–301, doi:10.1158/2159-8290.CD-18-0710 (2019). [PubMed: 30366930]

19. Elyada E et al. Cross-Species Single-Cell Analysis of Pancreatic Ductal Adenocarcinoma Reveals Antigen-Presenting Cancer-Associated Fibroblasts. Cancer Discov 9, 1102–1123, doi:10.1158/2159-8290.CD-19-0094 (2019). [PubMed: 31197017]
20. Tanne A et al. Distinguishing the immunostimulatory properties of noncoding RNAs expressed in cancer cells. Proceedings of the National Academy of Sciences 112, 15154–15159, doi:10.1073/pnas.1517584112 (2015).
21. Leonova KI et al. p53 cooperates with DNA methylation and a suicidal interferon response to maintain epigenetic silencing of repeats and noncoding RNAs. Proceedings of the National Academy of Sciences 110, E89–E98, doi:10.1073/pnas.1216922110 (2013).
22. Chiappinelli KB et al. Inhibiting DNA Methylation Causes an Interferon Response in Cancer via dsRNA Including Endogenous Retroviruses. Cell 162, 974–986, doi:10.1016/j.cell.2015.07.011 (2015). [PubMed: 26317466]
23. Roulois D et al. DNA-Demethylating Agents Target Colorectal Cancer Cells by Inducing Viral Mimicry by Endogenous Transcripts. Cell 162, 961–973, doi:10.1016/j.cell.2015.07.056 (2015). [PubMed: 26317465]
24. Canadas I et al. Tumor innate immunity primed by specific interferon-stimulated endogenous retroviruses. Nature medicine 24, 1143–1150, doi:10.1038/s41591-018-0116-5 (2018).
25. Grothey A et al. Regorafenib monotherapy for previously treated metastatic colorectal cancer (CORRECT): an international, multicentre, randomised, placebo-controlled, phase 3 trial. Lancet (London, England) 381, 303–312, doi:10.1016/s0140-6736(12)61900-x (2013).
26. Mayer RJ et al. Randomized trial of TAS-102 for refractory metastatic colorectal cancer. N Engl J Med 372, 1909–1919, doi:10.1056/NEJMoa1414325 (2015). [PubMed: 25970050]
27. Gilabert M et al. Evaluation of gemcitabine efficacy after the FOLFIRINOX regimen in patients with advanced pancreatic adenocarcinoma. Medicine (Baltimore) 96, e6544, doi:10.1097/md.0000000000006544 (2017). [PubMed: 28422841]
28. Dewan MZ et al. Fractionated but not single-dose radiotherapy induces an immune-mediated abscopal effect when combined with anti-CTLA-4 antibody. Clin Cancer Res 15, 5379–5388, doi:10.1158/1078-0432.Ccr-09-0265 (2009). [PubMed: 19706802]
29. Demaria S & Formenti SC Radiation as an immunological adjuvant: current evidence on dose and fractionation. Frontiers in oncology 2, 153, doi:10.3389/fonc.2012.00153 (2012). [PubMed: 23112958]
30. Schaue D, Ratikan JA, Iwamoto KS & McBride WH Maximizing tumor immunity with fractionated radiation. International journal of radiation oncology, biology, physics 83, 1306–1310, doi:10.1016/j.ijrobp.2011.09.049 (2012).
31. Verma V et al. PD-1 blockade in subprimed CD8 cells induces dysfunctional PD-1(+)CD38(hi) cells and anti-PD-1 resistance. Nat Immunol, doi:10.1038/s41590-019-0441-y (2019).
32. Rodriguez-Ruiz ME, Vitale I, Harrington KJ, Melero I & Galluzzi L Immunological impact of cell death signaling driven by radiation on the tumor microenvironment. Nature Immunology 21, 120–134, doi:10.1038/s41590-019-0561-4 (2020). [PubMed: 31873291]
33. Hindson J Radiation promotes systemic responses. Nature Reviews Immunology 19, 3–3, doi:10.1038/s41577-018-0102-7 (2019).
34. Dovedi SJ et al. Fractionated Radiation Therapy Stimulates Antitumor Immunity Mediated by Both Resident and Infiltrating Polyclonal T-cell Populations when Combined with PD-1 Blockade. Clin Cancer Res 23, 5514–5526, doi:10.1158/1078-0432.Ccr-16-1673 (2017). [PubMed: 28533222]
35. Hsiehchen D et al. DNA Repair Gene Mutations as Predictors of Immune Checkpoint Inhibitor Response beyond Tumor Mutation Burden. Cell Reports Medicine 1, 100034, doi:10.1016/j.xcrm.2020.100034 (2020). [PubMed: 32676589]
36. Solovyov A et al. Global Cancer Transcriptome Quantifies Repeat Element Polarization between Immunotherapy Responsive and T Cell Suppressive Classes. Cell Reports 23, 512–521, doi:10.1016/j.celrep.2018.03.042 (2018). [PubMed: 29642008]
37. Smith CC et al. Endogenous retroviral signatures predict immunotherapy response in clear cell renal cell carcinoma. The Journal of clinical investigation 128, 4804–4820, doi:10.1172/JCI121476 (2018). [PubMed: 30137025]

38. Rooney MS, Shukla SA, Wu CJ, Getz G & Hacohen N Molecular and genetic properties of tumors associated with local immune cytolytic activity. Cell 160, 48–61, doi:10.1016/j.cell.2014.12.033 (2015). [PubMed: 25594174]
39. Ting DT et al. Aberrant overexpression of satellite repeats in pancreatic and other epithelial cancers. Science 331, 593–596, doi:science.1200801 [pii] 10.1126/science.1200801 (2011). [PubMed: 21233348]
40. Desai N et al. Diverse repetitive element RNA expression defines epigenetic and immunologic features of colon cancer. JCI Insight 2, doi:10.1172/jci.insight.91078 (2017).
41. Kong Y et al. Transposable element expression in tumors is associated with immune infiltration and increased antigenicity. Nat Commun 10, 5228, doi:10.1038/s41467-019-13035-2 (2019). [PubMed: 31745090]
42. Zapatka M et al. The landscape of viral associations in human cancers. Nat Genet 52, 320–330, doi:10.1038/s41588-019-0558-9 (2020). [PubMed: 32025001]
43. Panda A et al. Endogenous retrovirus expression is associated with response to immune checkpoint blockade in clear cell renal cell carcinoma. JCI Insight 3, doi:10.1172/jci.insight.121522 (2018).
44. Quatrini L et al. The Immune Checkpoint PD-1 in Natural Killer Cells: Expression, Function and Targeting in Tumour Immunotherapy. Cancers (Basel) 12, doi:10.3390/cancers12113285 (2020).
45. Hsu J et al. Contribution of NK cells to immunotherapy mediated by PD-1/PD-L1 blockade. The Journal of clinical investigation 128, 4654–4668, doi:10.1172/jci99317 (2018). [PubMed: 30198904]
46. World Medical Association Declaration of Helsinki: ethical principles for medical research involving human subjects. Jama 310, 2191–2194, doi:10.1001/jama.2013.281053 (2013). [PubMed: 24141714]
47. Eisenhauer EA et al. New response evaluation criteria in solid tumours: revised RECIST guideline (version 1.1). European journal of cancer (Oxford, England : 1990) 45, 228–247, doi:10.1016/j.ejca.2008.10.026 (2009).
48. DePristo MA et al. A framework for variation discovery and genotyping using next-generation DNA sequencing data. Nat Genet 43, 491–498, doi:10.1038/ng.806 (2011). [PubMed: 21478889]
49. Van der Auwera GA et al. From FastQ data to high confidence variant calls: the Genome Analysis Toolkit best practices pipeline. Curr Protoc Bioinformatics 43, 11 10 11–11 10 33, doi:10.1002/0471250953.bi1110s43 (2013). [PubMed: 25431634]
50. Li H Aligning sequence reads, clone sequences and assembly contigs with BWA-MEM. arXiv: Genomics (2013).
51. Li H et al. The Sequence Alignment/Map format and SAMtools. Bioinformatics 25, 2078–2079, doi:10.1093/bioinformatics/btp352 (2009). [PubMed: 19505943]
52. McKenna A et al. The Genome Analysis Toolkit: a MapReduce framework for analyzing next-generation DNA sequencing data. Genome Res 20, 1297–1303, doi:10.1101/gr.107524.110 (2010). [PubMed: 20644199]
53. Cibulskis K et al. Sensitive detection of somatic point mutations in impure and heterogeneous cancer samples. Nat Biotechnol 31, 213–219, doi:10.1038/nbt.2514 (2013). [PubMed: 23396013]
54. Saunders CT et al. Strelka: accurate somatic small-variant calling from sequenced tumor-normal sample pairs. Bioinformatics 28, 1811–1817, doi:10.1093/bioinformatics/bts271 (2012). [PubMed: 22581179]
55. Tate JG et al. COSMIC: the Catalogue Of Somatic Mutations In Cancer. Nucleic Acids Res 47, D941–D947, doi:10.1093/nar/gky1015 (2019). [PubMed: 30371878]
56. Cingolani P et al. A program for annotating and predicting the effects of single nucleotide polymorphisms, SnpEff: SNPs in the genome of Drosophila melanogaster strain w1118; iso-2; iso-3. Fly (Austin) 6, 80–92, doi:10.4161/fly.19695 (2012). [PubMed: 22728672]
57. Grossman RL et al. Toward a Shared Vision for Cancer Genomic Data. N Engl J Med 375, 1109–1112, doi:10.1056/NEJMp1607591 (2016). [PubMed: 27653561]
58. Newman AM et al. Determining cell type abundance and expression from bulk tissues with digital cytometry. Nature Biotechnology 37, 773–782, doi:10.1038/s41587-019-0114-2 (2019).

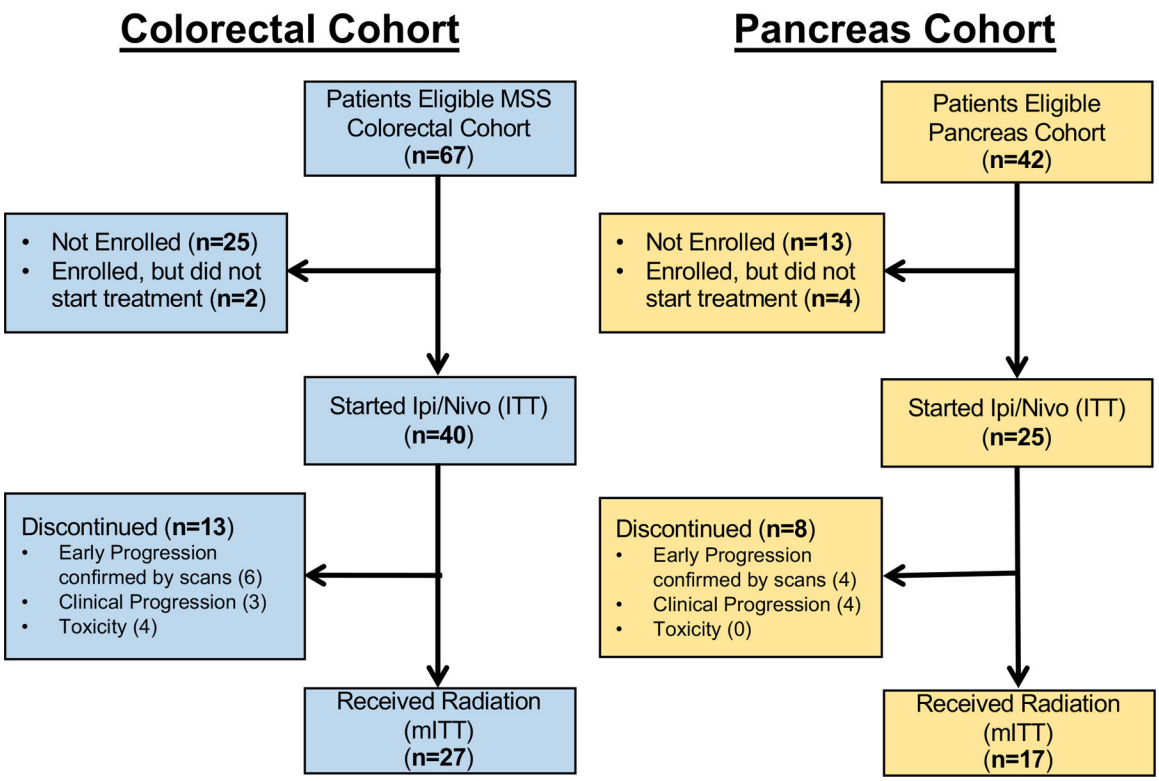

Fig. 1. Consort diagram of enrolled patients.

Shown are the patients that were enrolled for intention to treat (ITT) and those who received radiation (per-protocol). The n shown represents the number of patients at each stage of the protocol.

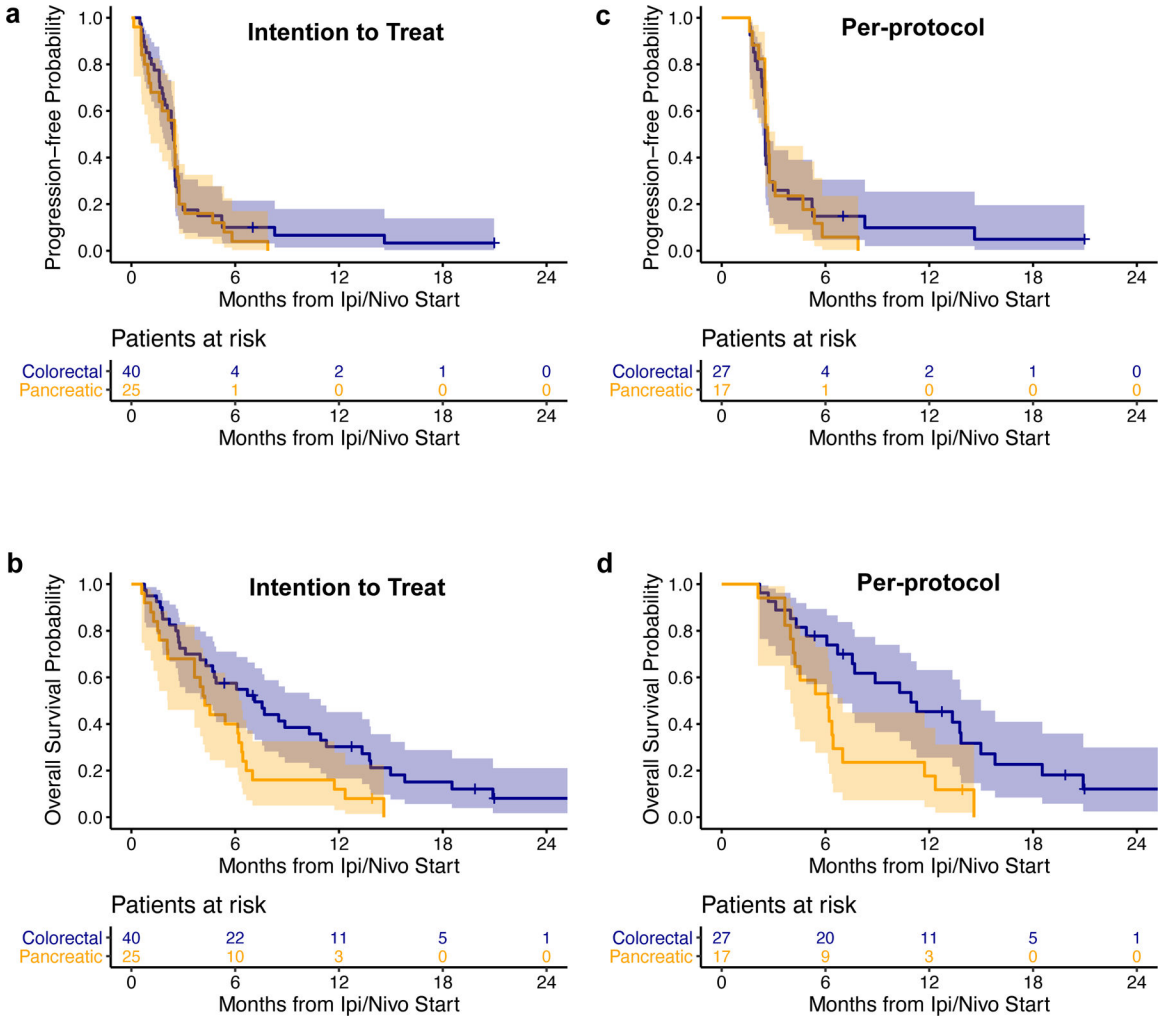

Fig. 2. Progression-free and overall survival analysis.

a, b, Kaplan-Meier curve of progression-free survival (**a**) and overall survival (**b**) of patients in ITT cohort. The CRC cohort (n = 40; blue) had a median PFS 2.4 months and median OS of 7.1 months. The PDAC cohort (n = 25; orange) had a median PFS of 2.5 months and median OS of 4.2 months. 95% confidence intervals shown.

c, d, Kaplan-Meier curve of progression-free survival (**c**) and overall survival (**d**) of patient in per-protocol cohort. The CRC cohort (n = 27; blue) had a median PFS of 2.5 months and median OS of 10.9 months. The PDAC cohort (n = 17; orange) had a median PFS of 2.7 months and median OS of 6.1 months. 95% confidence intervals shown.

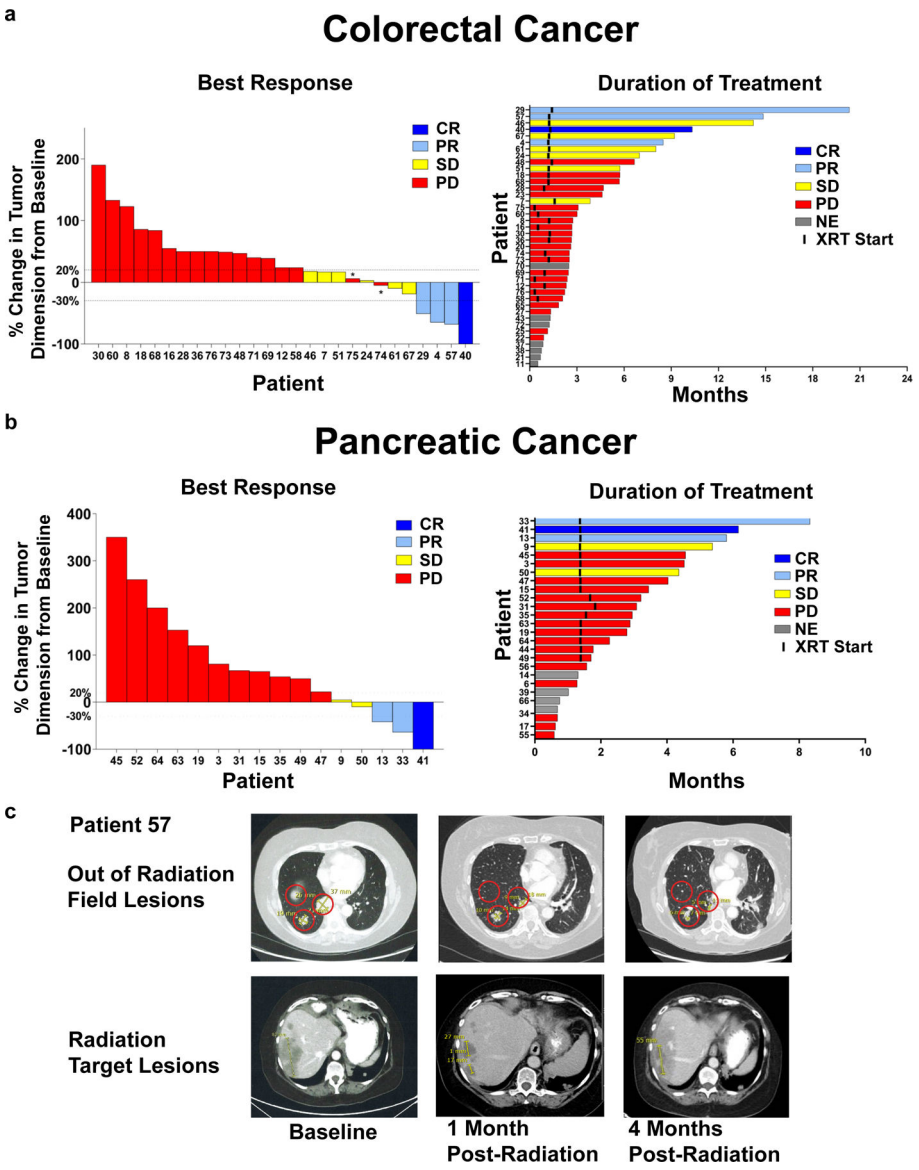

Fig. 3. Response to treatment by change in measurable disease.

a, Percent (%) change in tumor dimension of comparable lesion(s) at best response for the per-protocol colorectal cancer cohort and duration of treatment for the ITT colorectal cancer cohort.

b, Percent (%) change in tumor dimension of comparable lesion(s) at best response for the per-protocol pancreatic cancer cohort and duration of treatment for the ITT pancreatic cancer cohort.

Bars color coded for responders (SD – yellow, PR/CR – blue) and non-responders (PD. – red). Non-evaluable (NE - gray) and XRT (radiotherapy) start time (black bar). Of note: patient #44 received radiation but progressed prior to scans. *unequivocal PD due to new metastatic lesions

c, Example of response in Patient 57 with 3 lung metastases that responded after radiation treatment of the target lesion in the liver with combined ipilimumab and nivolumab

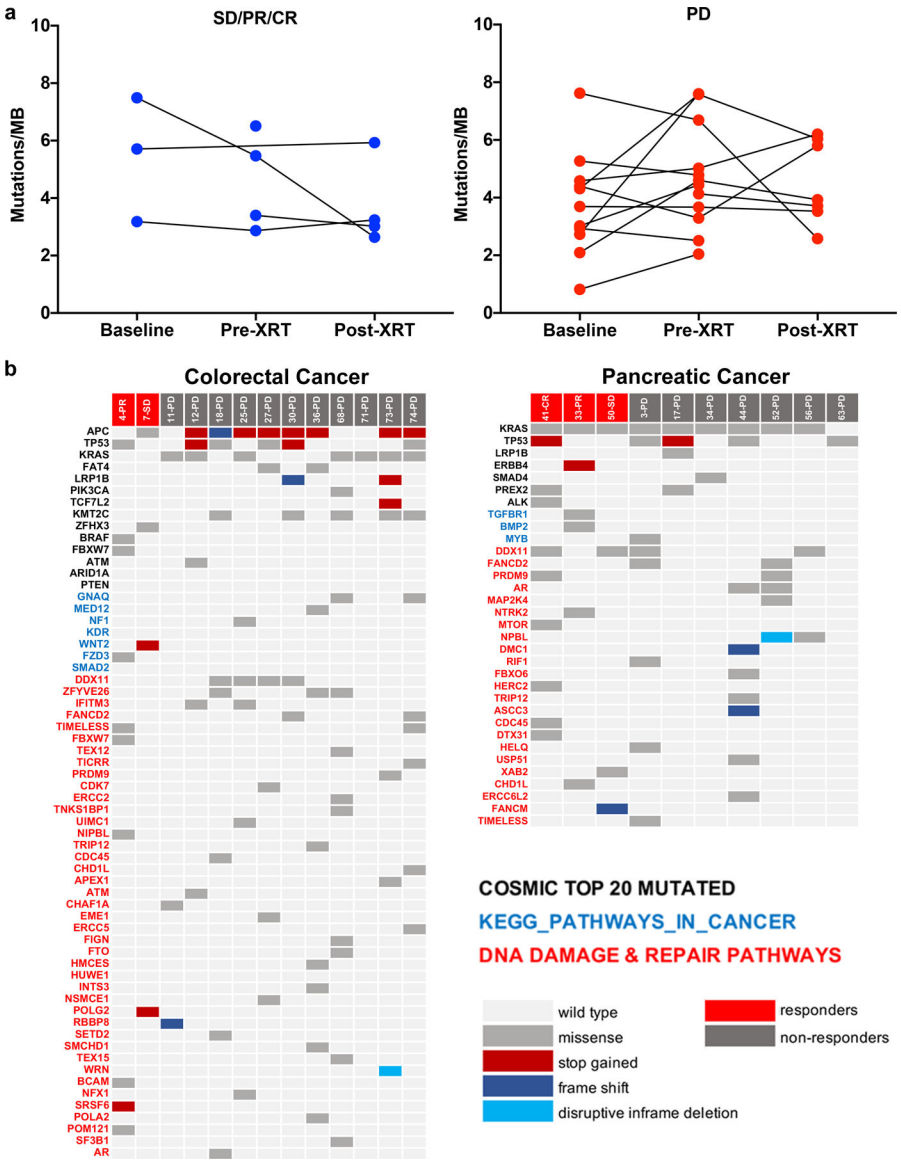

Fig. 4. Tumor mutational burden and exome mutations in patient biopsies.

a, Tumor mutational burden (TMB) measured in mutations per megabase (MB) in baseline, Pre-XRT, Post-XRT biopsies. In patients with response (left: SD/PR/CR; n = 5) and progressive disease (right: PD; n = 12).

b, Curated non-synonymous mutations in whole exome sequencing of colorectal and pancreatic cancer biopsies listing most commonly mutated genes from COSMIC (black), KEGG_PATHWAYS_IN_CANCER (blue), and DNA DAMAGE & REPAIR PATHWAYS (red). Mutation type color coded in legend and responders (SD/PR/CR) in red and non-responders (PD) in gray.

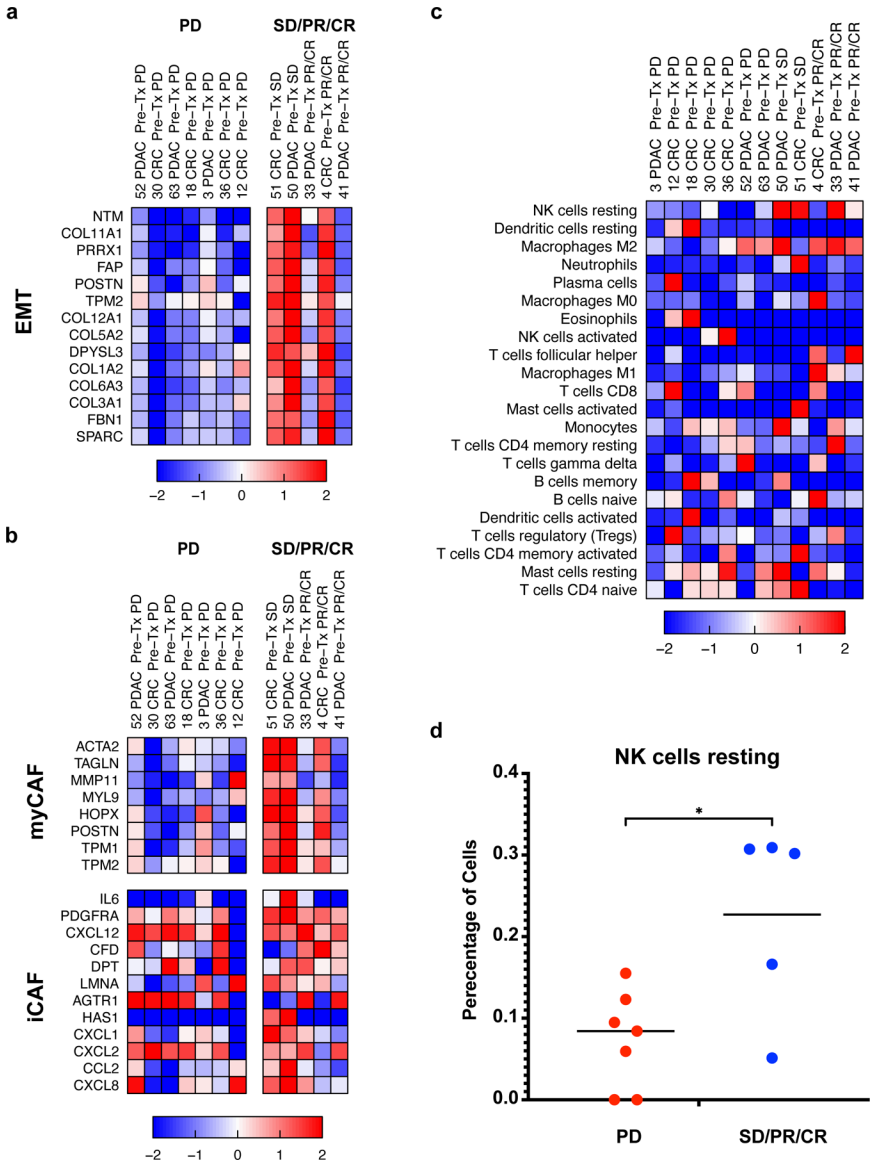

Fig. 5. Coding gene RNA expression and immune cell differences in patient biopsies.

a, RNA-seq heatmap of EMT genes found statistically significant (FDR < 0.05) in pretreatment (Pre-Tx) biopsies enriched in patients with response (SD/PR/CR; n = 5) compared to progressive disease (PD; n =7). Scale −2 to 2 represents minimum and maximum values within the heatmap.

b, RNA-seq heatmap of myCAF and iCAF genes in Pre-Tx biopsies in patients with SD/PR/CR (n = 5) compared to PD (n =7). Scale −2 to 2 represents minimum and maximum values within the heatmap.

c, Immune infiltrate analysis using CIBERSORTx deconvolution in patient biopsies shown as heatmap of cell percentage of immune cells in pre-treatment biopsies from patients with SD/PR/CR (n = 5) and PD (n =7).

d, Dot plot of resting NK cell percentage in pre-treatment biopsies between SD/PR/CR (n = 5) and PD (n =7) that was statistically significant * 2-tailed unpaired t-test p = 0.038.

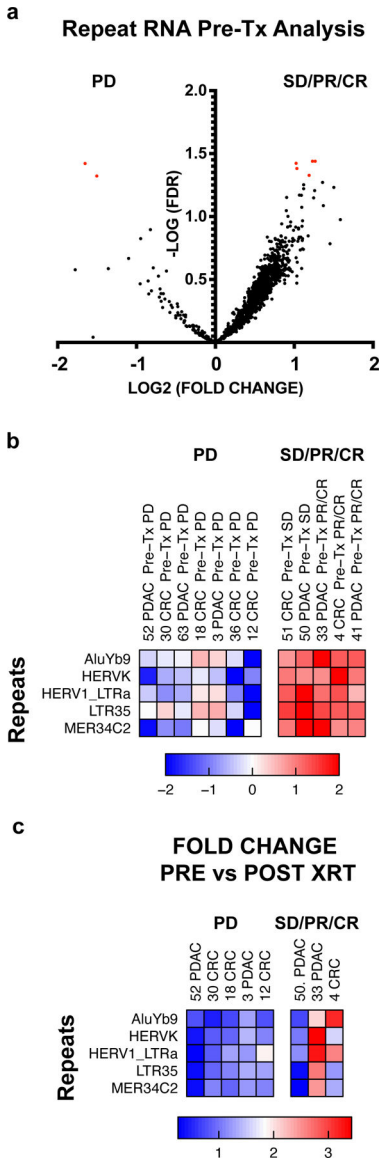

Fig. 6. Repeat RNA expression differences in patient biopsies.

a, Volcano plot of repeat RNAs in comparing Pre-Tx biopsies in patients with SD/PR/CR compared to PD. Y-axis = − log10 (FDR) and x-axis = log2 (Fold change).

b, RNA-seq heatmap of repeat RNA genes found statistically significant (FDR < 0.05) in Pre-Tx biopsies enriched in patients with SD/PR/CR (n = 5) compared to PD (n = 7). Scale −2 to 2 represents minimum and maximum values within the heatmap.

c, Fold change of significant repeat RNAs in Pre-XRT compared to Post-XRT samples available for analysis for SD/PR/CR (n = 3) and PD (n =5). Higher fold change with increasing red.

Table 1.

Baseline patient and disease characteristics

	Colorectal	Pancreas
Characteristic	N = 40	N = 25
Median age, years (range)	59 (26–83)	60 (32–75)
Race		
White	38 (95%)	23 (92%)
Black/Asian/Other	2 (5%)	2 (8%)
Male Sex	22 (55%)	18 (72%)
ECOG PS		
0	26 (65%)	11 (44%)
1	14 (35%)	14 (56%)
Median Number of Prior Regimens (including Chemotherapy and ChemoRT) (range)	4 (1–13)	2 (1–4)
Stage at Diagnosis		
Upfront Resectable	17 (42%)	6 (24%)
Borderline *(PDAC only)*	N/A	1 (4%)
Locally Advanced *(PDAC only)*	N/A	7 (28%)
Metastatic	23 (58%)	11 (44%)
Median Time from Diagnosis to C1D1 (Months) (range)	44.9 (7.2–198.7)	16.9 (3.7–54.8)

C1D1, day 1 of cycle 1; chemoRT, chemoradiotherapy; N/A, not applicable.

Table 2.

Efficacy by best overall response

Efficacy				
	Colorectal		Pancreas	
	ITT (N=40)	Per-protocol (N=27)	ITT (n=25)	Per-protocol (n=17)
ORR	4 (10%)	4 (15%)	3 (12%)	3 (18%)
DCR	10 (25%)	10 (37%)	5 (20%)	5 (29%)
Discontinued due to toxicity[a,b]	4 (10%)	1 (4%)	1 (4%)	1 (6%)
Progression free survival (median in months)	2.4	2.5	2.5	2.7
Overall survival (median in months)[c]	7.1	10.9	4.2	6.1

[a.] Colorectal cohort discontinuation prior to XRT (radiotherapy): toxicity (4), progression confirmed by scans (6), clinical progression (3)

[b.] Pancreas cohort discontinuation prior to XRT: toxicity (0), progression confirmed by scans (4), clinical progression (4)

[c.] Colorectal cohort: 6 patients alive with median follow-up of 16.6 months (range 5.4–28.0); Pancreas cohort: 1 patient alive at 13.9 months